



**HAL**  
open science

## Identifying G-Quadruplex-DNA-Disrupting Small Molecules

Jérémie Mitteau, Pauline Lejault, Filip Wojciechowski, Alexandra Joubert, Julien Boudon, Nicolas Desbois, Claude P Gros, Robert H E Hudson, Jean-Baptiste Boulé, Anton Granzhan, et al.

► **To cite this version:**

Jérémie Mitteau, Pauline Lejault, Filip Wojciechowski, Alexandra Joubert, Julien Boudon, et al.. Identifying G-Quadruplex-DNA-Disrupting Small Molecules. *Journal of the American Chemical Society*, 2021, 143 (32), pp.12567-12577. 10.1021/jacs.1c04426 . hal-03321473

**HAL Id: hal-03321473**

**<https://hal.science/hal-03321473>**

Submitted on 18 Aug 2021

**HAL** is a multi-disciplinary open access archive for the deposit and dissemination of scientific research documents, whether they are published or not. The documents may come from teaching and research institutions in France or abroad, or from public or private research centers.

L'archive ouverte pluridisciplinaire **HAL**, est destinée au dépôt et à la diffusion de documents scientifiques de niveau recherche, publiés ou non, émanant des établissements d'enseignement et de recherche français ou étrangers, des laboratoires publics ou privés.

## Identifying G-Quadruplex-DNA-Disrupting Small Molecules

Jérémie Mitteau, Pauline Lejault, Filip Wojciechowski, Alexandra Joubert, Julien Boudon, Nicolas Desbois, Claude Gros, Robert Hudson, Jean-Baptiste Boulé, Anton Granzhan, et al.

► **To cite this version:**

Jérémie Mitteau, Pauline Lejault, Filip Wojciechowski, Alexandra Joubert, Julien Boudon, et al.. Identifying G-Quadruplex-DNA-Disrupting Small Molecules. *Journal of the American Chemical Society*, American Chemical Society, 2021, 10.1021/jacs.1c04426 . hal-03321473

**HAL Id: hal-03321473**

**<https://hal.archives-ouvertes.fr/hal-03321473>**

Submitted on 18 Aug 2021

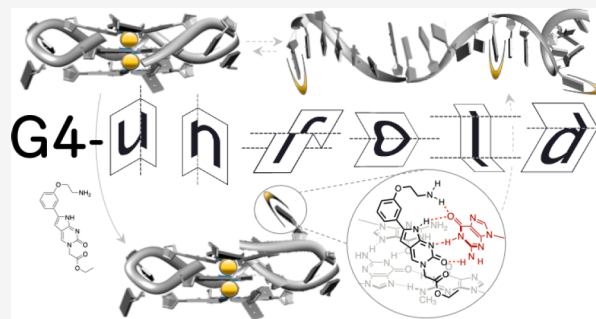
**HAL** is a multi-disciplinary open access archive for the deposit and dissemination of scientific research documents, whether they are published or not. The documents may come from teaching and research institutions in France or abroad, or from public or private research centers.

L'archive ouverte pluridisciplinaire **HAL**, est destinée au dépôt et à la diffusion de documents scientifiques de niveau recherche, publiés ou non, émanant des établissements d'enseignement et de recherche français ou étrangers, des laboratoires publics ou privés.

# Identifying G-Quadruplex-DNA-Disrupting Small Molecules

J r mie Mitteau, Pauline Lejault, Filip Wojciechowski, Alexandra Joubert, Julien Boudon, Nicolas Desbois, Claude P. Gros, Robert H. E. Hudson, Jean-Baptiste Boul , Anton Granzhan, and David Monchaud\*

**ABSTRACT:** The quest for small molecules that strongly bind to G-quadruplex-DNA (G4), so-called G4 ligands, has invigorated the G4 research field from its very inception. Massive efforts have been invested to discover or rationally design G4 ligands, evaluate their G4-interacting properties in vitro through a series of now widely accepted and routinely implemented assays, and use them as innovative chemical biology tools to interrogate cellular networks that might involve G4s. In sharp contrast, only uncoordinated efforts aimed at developing small molecules that destabilize G4s have been invested to date, even though it is now recognized that such molecular tools would have tremendous application in neurobiology as many genetic and age-related diseases are caused by an overrepresentation of G4s. Herein, we report on our efforts to develop in vitro assays to reliably identify molecules able to destabilize G4s. This workflow comprises the newly designed G4-unfold assay, adapted from the G4-helicase assay implemented with Pif1, as well as a series of biophysical and biochemical techniques classically used to study G4/ligand interactions (CD, UV-vis, PAGE, and FRET-melting), and a qPCR stop assay, adapted from a *Taq*-based protocol recently used to identify G4s in the genomic DNA of *Schizosaccharomyces pombe*. This unique, multipronged approach leads to the characterization of a phenylpyrrolocytosine (PhpC)-based G-clamp analog as a prototype of G4-disrupting small molecule whose properties are validated through many different and complementary in vitro evaluations.



## INTRODUCTION

The existence of a higher order, four-stranded DNA structure known as G-quadruplex-DNA (G4-DNA or G4)<sup>1-4</sup> within functional human cells is now established through different technologies, including structure-specific isolation and identification techniques (either low-<sup>5,6</sup> or high-throughput techniques)<sup>7-10</sup> and optical imaging.<sup>3,11,12</sup> The cellular role of G4s defies easy understanding and explanations since G4s fold from numerous regions of the human genome (>500 000)<sup>2,13,14</sup> that are not systematically committed to key regulatory functions. However, their formation is unquestionably coupled with DNA transactions (transcription and replication)<sup>15-18</sup> as a result of both duplex melting and supercoiling originating in the motion of DNA/RNA polymerases along the duplex stem. This makes G4 formation a possible impediment to DNA transactions as G4s possess high thermodynamic stability and may be persistent in genomic DNA, therefore representing solid physical obstacles to helicase and polymerase processivity.

To prevent such a situation, DNA/RNA polymerases coordinate their action with enzymes that unwind G4s, known as G4-helicases.<sup>19-23</sup> The uncoupling of the polymerase and helicase activity creates a crisis situation that ultimately leads to DNA damage and genome instability. This might arise as a result of either an abnormal G4 stabilization (for instance,

via externally added G4-stabilizing compounds, or G4 ligands) or a G4-helicase impairment. This later hypothesis is now well documented as the loss-of-function mutation of helicases is linked to severe genetic conditions. Numerous human helicases have been characterized belonging to two different helicase superfamilies (SF1 and SF2),<sup>24,25</sup> which include the SF1 Pif1,<sup>26-28</sup> the SF2 BLM,<sup>29,30</sup> and WRN<sup>30,31</sup> (RecQ-like helicase subfamily) as well as FANCF<sup>32,33</sup> and DDX1<sup>34,35</sup> (Fe-S helicase subfamily). Each of these enzymes is associated with a human genetic disease: Bloom syndrome (growth retardation, immunodeficiency) is caused by a mutation of BLM,<sup>36</sup> Werner syndrome (adult progeria) by that of WRN,<sup>37</sup> Fanconi anemia (developmental abnormalities, bone marrow failure) by FANCF,<sup>38-40</sup> and Warsaw Breakage syndrome (impaired growth, intellectual disability) by DDX1.<sup>34,41</sup> Pif1 deficiency is more generally associated with cancer predisposition.<sup>42</sup> Also, we recently showed that an overrepresenta-

Received: April 28, 2021

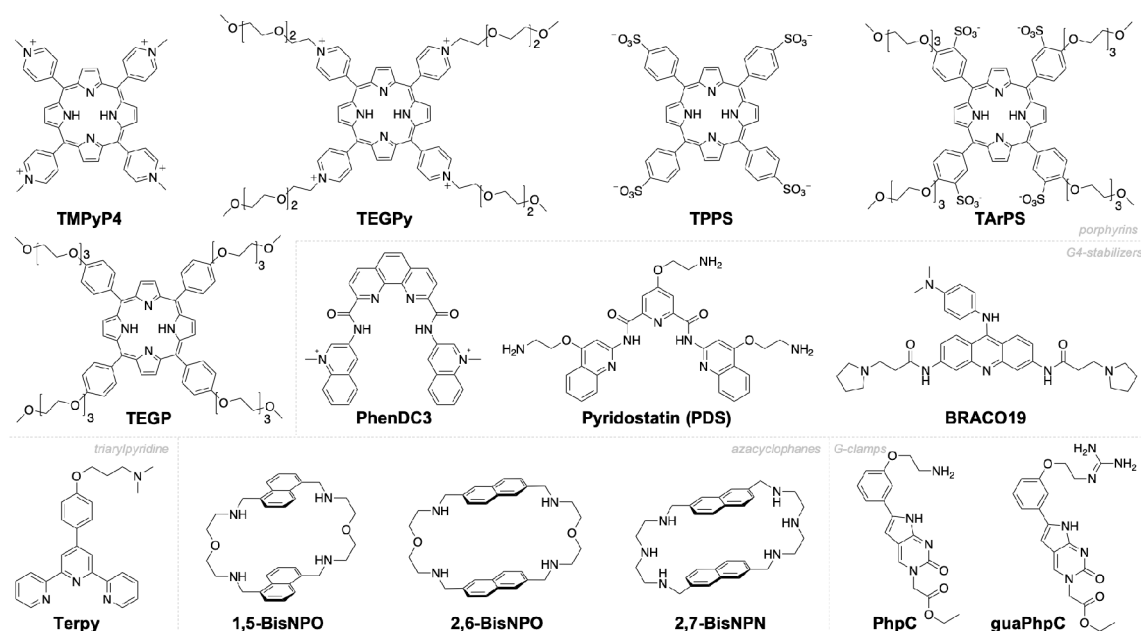


**Figure 1.** Molecules evaluated in the G4-unfold assay belonging to a series of porphyrins (TMPyP4, TEGPy, TPPS, TArPS, and TEGP), G4 stabilizers (PhenDC3, PDS, and BRACO19), triarylpyridines (Terpy), azacyclophanes (1,5-BisNPO, 2,6-BisNPO, and 2,7-BisNPN), and G-clamp analogues (PhpC and guaPhpC).

tion of G4s originating in either age-associated changes in the activity of G4-modulating proteins or in G4 stabilization by G4 ligands may accelerate brain aging and foster neurological disorders.<sup>43</sup>

In light of this, it is surprising that most, if not all, chemical biology efforts have been invested in the quest for chemicals that stabilize G4s (G4 ligands)<sup>44</sup> rather than compounds capable of unfolding G4s to rescue helicase impairment.<sup>23</sup> Beyond historical reasons (the first therapy-oriented G4 ligand was reported in 1997 to stabilize telomeric G4 in order to impair the cancer-relevant telomerase enzymatic complex),<sup>45</sup> G4 stabilization can be a strategic way to inflict severe damage to the genome of cancer cells, the selectivity of the treatment relying on their flawed repertoire of DNA damage signaling and repair capabilities (collectively known as DNA damage response, or DDR) as compared to healthy cells.<sup>17</sup> However, this does not explain the paucity of validated prototypes of G4 unwinders, which could be applied to pathological G4 formation.

Over the past years, some examples of G4 unwinders have been reported,<sup>23,46,47</sup> such as the porphyrin TMPyP4, shown to unfold G4-DNA that folds from d[(CG<sub>2</sub>)<sub>n</sub>] trinucleotide repeats, whose expansion is involved in the Fragile X syndrome,<sup>48,49</sup> from the d[(G<sub>4</sub>C<sub>2</sub>)<sub>n</sub>] hexanucleotide repeats, whose expansion is linked to ALS/FTD,<sup>50</sup> and also the thrombin binding aptamer (TBA) G4.<sup>51</sup> Other examples include an anthrathiophenedione derivative, shown to unfold the human telomeric G4-forming sequence d[(TTAGGG)<sub>n</sub>],<sup>52</sup> the triarylpyridine TAPI, reported to disrupt the G4 that folds from a sequence of the c-kit promoter;<sup>53</sup> a series of stiff-stilbenes found to regulate the folding/unfolding of the telomeric G4 in a photoresponsive manner;<sup>54</sup> along with copper ion and copper complexes,<sup>55,56</sup> urea,<sup>57,58</sup> and natural polyamines (e.g., spermine).<sup>59</sup> There is, however, not broad consensus on the use of these chemicals as surrogates for helicases given that no in-depth cellular investigations have been yet performed. This might be due to the doubts about

their actual unfolding activity: TMPyP4 is an illustrative example of this conundrum, as it was studied for more than two decades as a G4 stabilizer<sup>44,60–62</sup> and is now reported as a G4 unfold.<sup>48–51,63–66</sup> These surprising results are however in line with previous reports in which the paradoxical behavior of porphyrin derivatives is described, either as a function of the nature of their metallic complexes (the platinum complex of TMPyP4 destabilizes G4s, while the free base TMPyP4 and both the zinc and the copper complexes stabilize them)<sup>67</sup> or as a function of the techniques implemented (the spermine-decorated porphyrin TCPPSpm4 can destabilize or stabilize G4s if gradual or blunt additions are performed, respectively).<sup>68</sup>

We reasoned that a possible problem is the lack of reliable in vitro assays to assess the G4-unfolding properties of chemicals. Dozens of assays have been developed to quantify the G4-stabilizing properties of ligands;<sup>69,70</sup> in sharp contrast, no reliable, systematic, and high-throughput screening (HTS) assay is available for studying G4 disruption. The candidates for G4 unwinding described above were identified via different low-throughput assays, chiefly polyacrylamide gel electrophoresis (PAGE) and circular dichroism (CD), without systematic comparison and analysis of suited controls. Some attempts have also been made to transpose in vitro assays developed for assessing G4-stabilizing agents to the quest for G4 unwinders (e.g., FRET-melting assay), but their reliability was not cross-checked by systematic comparison with other techniques. Here, we tackle these issues, combining 8 different techniques (G4-unfold, CD, UV-vis, PAGE, DLS, FRET-melting, G4-helicase assay, and qPCR stop assay, vide infra) in a single workflow that leads to the identification of a prototype of G4 unwinder, PhpC, whose properties are thus validated according to multiple and complementary indicators.

## RESULTS AND DISCUSSION

**Representative Panel of Candidates.** We first selected a panel of 14 representative candidates (Figure 1) to be studied

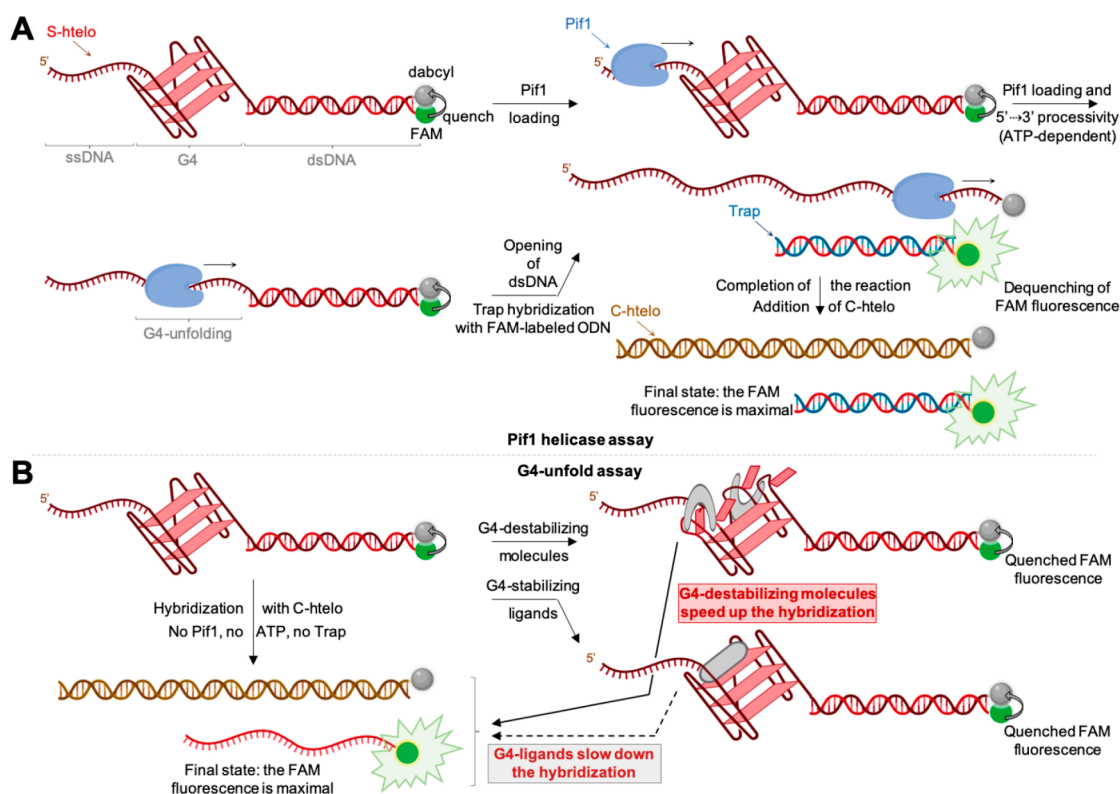


**Figure 2.** Schematic representation of the helicase assay developed by Mendoza, Bourdoncle, et al.<sup>90</sup> (A) and of the related G4-unfold assay suited to evaluate the G4-destabilizing properties of small molecules (B). Created with BioRender.

for their stabilizing/unfolding properties. This panel comprised five porphyrins including the tetracationic TMPyP4<sup>48–51,60–66</sup> and its PEGylated analogue TEGPy,<sup>71,72</sup> the tetraanionic TPPS and its PEGylated analogue TArPS,<sup>73</sup> and the neutral, water-soluble (PEGylated) TEGP. These porphyrins were selected to assess both the actual efficiency of TMPyP4 and the influence of charge (cationic, neutral, anionic) and PEG arms on the G4-disruption/stabilization ability of the porphyrin scaffold. We also included three G4 ligands, PhenDC3,<sup>74,75</sup> PDS,<sup>76,77</sup> and BRACO19,<sup>78–80</sup> to calibrate the assay with firmly established G4 stabilizers. We also added a TAPI<sup>53,81</sup> analogue referred to as Terpy, initially used as a negative control for TAPI and used here to assess the actual performance of this terpyridine scaffold under a different experimental setup. We also selected a series of compounds that might be suited to G4 disruption, i.e., three macrocyclic bis-naphthalene compounds (or azacyclophanes), 1,5-BisNPO, 2,6-BisNPO, and 2,7-BisNPN,<sup>82–84</sup> whose ability to sandwich and stabilize isolated aromatic compounds (ideally here, a wobbling guanine escaping from the external G-quartet upon G4 destabilization) has been demonstrated by both NMR<sup>85</sup> and X-ray crystal structure analysis,<sup>86</sup> and two G-clamp<sup>87</sup> analogues, PhpC and guaPhpC,<sup>88,89</sup> known to strongly interact with Gs thanks to the formation of 4 H bonds (versus 3 in the canonical GC base pair), which could similarly trap and stabilize a flipping guanine.

**First Selection Step: G4-Unfold Assay.** We first focused on the fluorescence-based helicase assay developed by Mendoza, Bourdoncle et al. in which the G4-opening ability of the helicase Pif1 was quantified via a HTS-compatible fluorescence analysis (Figure 2A).<sup>90</sup> This assay is efficient but, in its present state, cannot be conveniently used as a HTS test for screening G4-disrupting molecules, mostly because of the

limited access to Pif1 helicase (not commercially available; it must be expressed and purified). We reasoned that a simplified version of this assay might be suited to assess the G4-disrupting activity of small molecules. In the original setup, the substrate of Pif1 is a bimolecular DNA system named S-htelo (Table S1), made of a 49-nt long oligodeoxynucleotide (ODN) that includes a 5' d<sup>[5'(A)<sub>11</sub>3']</sup> tail for Pif1 loading, the human telomeric sequence d<sup>[5'(G<sub>3</sub>T<sub>2</sub>A)<sub>3</sub>G<sub>3</sub>3']</sup>, and a 17-nt 3' tail labeled with dabcyl (consequently named dabcyl-labeled 49-nt ODN), and a 15-nt long ODN that is complementary to the 3' tail of the dabcyl-labeled 49-nt ODN and labeled with FAM on its 5'-end (consequently named FAM-labeled 15-nt ODN). When hybridized, this system possesses a single-stranded region (for helicase loading), a folded G4, and a duplex region that ends with a FRET pair in which the FAM fluorescence is quenched by the proximal dabcyl. The helicase assay per se is triggered by the addition of Pif1 that unfolds the system in a 5' to 3' direction in the presence of ATP. Strand separation is then monitored through the enhancement of the FAM fluorescence. The possible rehybridization is suppressed by the addition of a 15-nt ODN named Trap (5 mol equiv), complementary to the FAM-labeled 15-nt ODN, and the process is driven to completion by the addition of a 49-nt ODN named C-htelo (5 mol equiv), fully complementary to dabcyl-labeled 49-nt ODN. This assay was originally developed to quantify Pif1 activity and its inhibition by G4-stabilizing agents (BRACO-19,<sup>78</sup> pyridostatin (PDS),<sup>76</sup> PhenDC3,<sup>74</sup> and TrisQ,<sup>91</sup> 25 mol equiv).

The bottleneck of this assay being the accessibility of Pif1, we reasoned that the kinetics of the final DNA system opening upon addition of C-htelo could be an adequate and sufficient output. This kinetics could be affected by the presence of chemicals, being either slowed down by G4-stabilizing

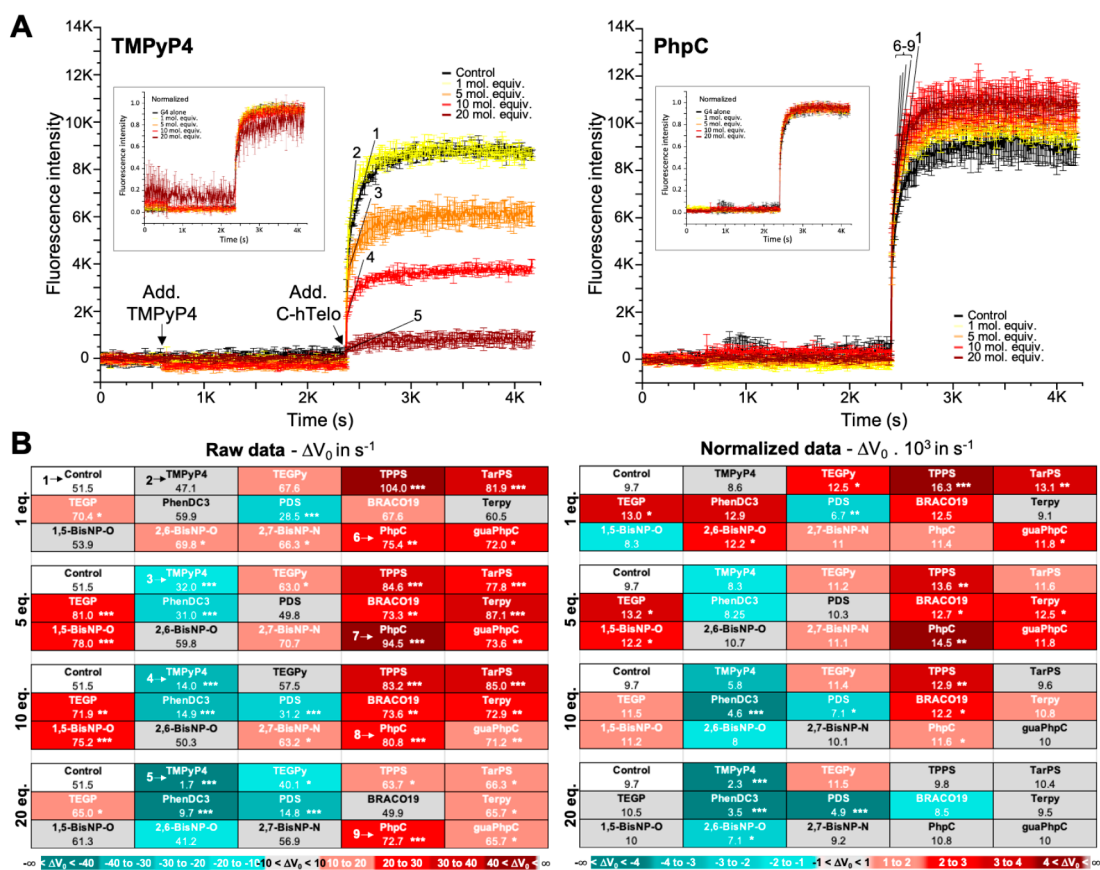


**Figure 3.** (A) Examples of experimental curves ( $n = 2$ ) obtained for G4-unfold investigations performed with increasing amounts (1–20 mol equiv) of TMPyP4 (left panel) and PhpC (right panel). (Insets) Corresponding normalized curves. (B) Heat maps of averaged initial velocity values ( $V_0$ , in  $s^{-1}$ ) obtained when performing the G4-unfold assay with 14 ligands at 4 different concentrations (from 1 to 20 mol equiv,  $n > 4$ ) with either raw data (left panel) or normalized data (right panel); values toward dark red are above the control ( $V_0 = 51.5 s^{-1}$ ), and those toward dark cyan are below the control. Significance determined by two-sample  $t$  test: \*  $p < 0.01$ , \*\*  $p < 0.001$ , and \*\*\*  $p < 0.0001$ .

compounds or accelerated by G4-destabilizing compounds. This approach would greatly simplify the protocol, making it a two-step/one-pot assay in which the initial FAM/dabcyl duplex is incubated with putative candidates whose effect on G4 stability is directly monitored upon addition of C-helo (no Pif1, no ATP, no Trap). This assay that we named G4-unfold (Figure 2B) is practically convenient as it can be performed at room temperature in 1 h in a 96-well plate format.

We evaluated the effect of the 14 candidates at 4 different concentrations (1, 5, 10, and 20 mol equiv, Figures 3 and S1–S10, Table S2), monitoring the variation in double strand hybridization kinetics by calculating the initial velocity of hybridization ( $V_0$ ,  $n > 4$ ). For the 14 candidates, a wide range of  $V_0$  values was obtained, between 1.7 and 104.0  $s^{-1}$  distributed around that of the control (performed without ligand,  $V_0 = 51.5 s^{-1}$ ). The presence of small molecules affects both the kinetics (represented by the slope of the curve seen in Figure 3A after C-hTelo addition) and the thermodynamics of the hybridization (represented by the final fluorescence level). This can be taken into account by analyzing either raw or normalized data (see insets in Figure 3A) or both: variations in  $V_0$  values, represented as heat maps seen in Figure 3B, clearly distinguish the G4-destabilizing (red) from the G4-stabilizing candidates (cyan), from both raw (left panel) and normalized data (right panel). Both PDS and PhenDC3 markedly slow down the hybridization (with  $V_0$  (raw data) down to 14.8 and 9.7  $s^{-1}$ , respectively), thus lending credence to the hypothesis

that G4 stabilization leads to low  $V_0$  values. From this point of view, TMPyP4 is clearly categorized as a G4-stabilizing ligand (with  $V_0 = 47.1, 32.0, 14.0$ , and  $1.7 s^{-1}$  for 1, 5, 10, and 20 mol equiv, respectively), more efficient than BRACO19 (with  $V_0 > 49.9 s^{-1}$ ). Conversely, the tetra-anionic porphyrins help hybridization (with  $V_0$  up to 104.0  $s^{-1}$ ), thus demonstrating that the charge of the porphyrins matters: while cationic porphyrins stabilize G4 particularly at elevated concentrations (with  $V_0 = 1.7$  and  $40.1 s^{-1}$  at 20 mol equiv of TMPyP4 and TEGPy, respectively), the negatively charged porphyrins accelerate hybridization, particularly at low concentrations ( $V_0 = 104.0$  and  $81.9 s^{-1}$  at 1 mol equiv of TPPS and TArPS, respectively). They are less efficient at elevated concentrations (with  $V_0 = 63.7$  and  $66.3 s^{-1}$  at 20 mol equiv of TPPS and TArPS, respectively), likely due to the growing contribution of the stabilizing,  $\pi$ -stacking interaction of the porphyrin scaffold with the G4 core. The other candidates moderately accelerate the hybridization (with  $V_0$  between 65.0 and 81.0, 60.5 and 87.1, 53.9 and 78.0, 56.9 and 70.7, and 65.7 and  $73.6 s^{-1}$  for TEGP, Terpy, 1,5-BisNPO, 2,7-BisNPN, and guaPhpC, respectively) with the notable exception of PhpC that helps hybridization quite efficiently over the whole concentration range (with  $V_0$  between 72.7 and  $94.5 s^{-1}$ ).

**Bulk of In Vitro Assays: CD, UV-vis, PAGE, DLS, FRET-Melting, and Fluorescence Investigations.** We further investigated the G4-interacting properties of a panel of selected compounds, i.e., TMPyP4 and PhenDC3 as stabilizers and

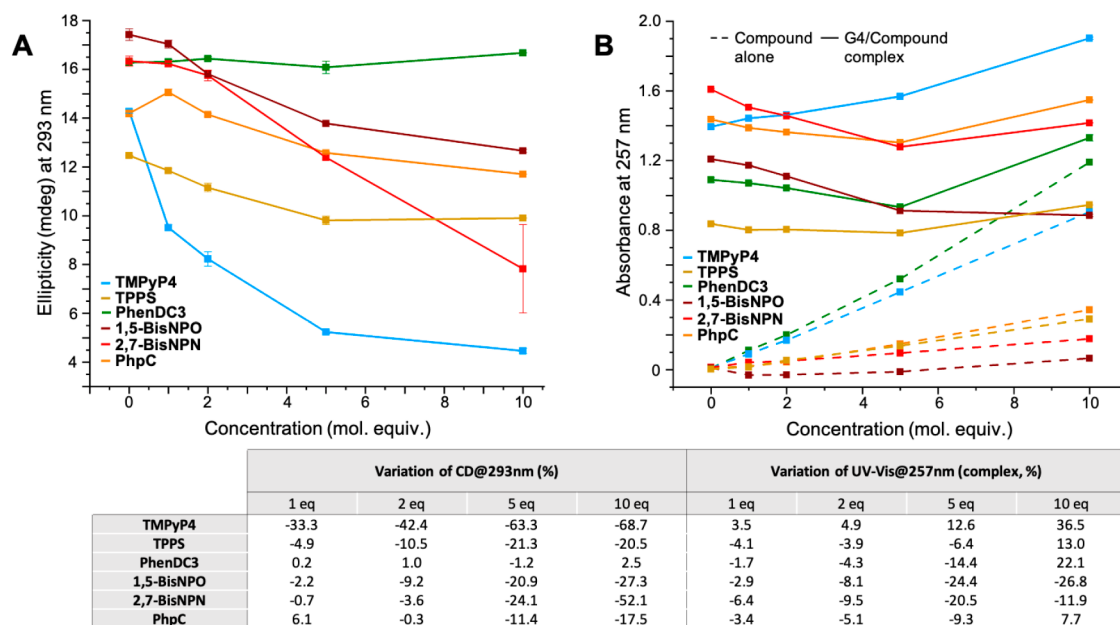


**Figure 4.** CD (A) and UV–vis titrations (B) of hTelo G4 (3  $\mu$ M) with increasing amounts (0–10 mol equiv) of 6 compounds (TMPyP4, TPPS, PhenDC3, 1,5-BisNPO, 2,7-BisNPN, and PhpC). Summary of the variations observed in the CD and UV–vis titrations performed with increasing amounts of the 6 compounds.

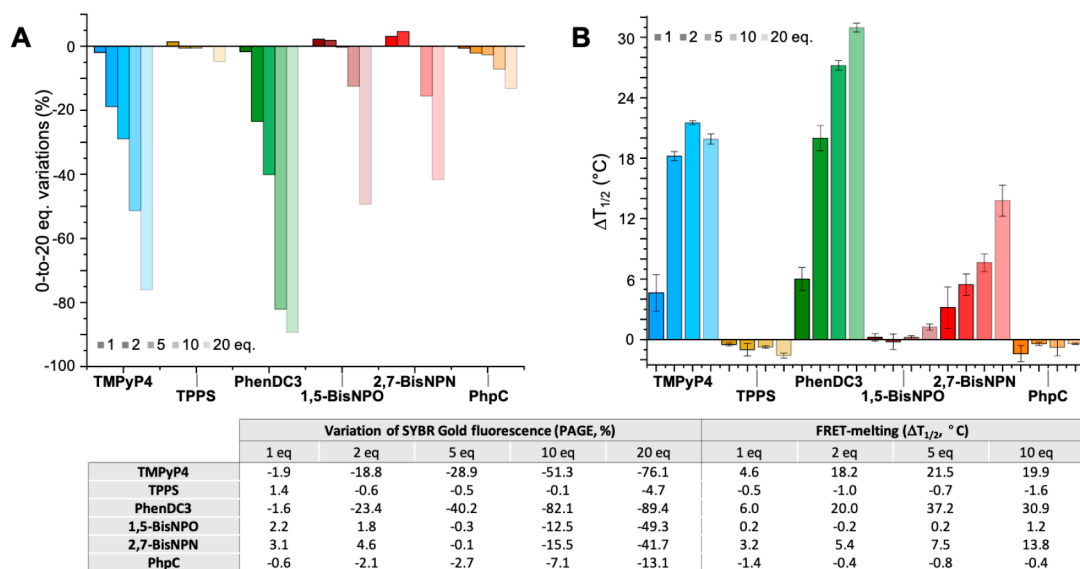


**Figure 5.** (A) Quantification (variation of SYBR Gold fluorescence) of PAGE experiments ( $n = 2$ ) performed with hTelo and increasing amounts (0–20 mol equiv) of 6 compounds (TMPyP4, TPPS, PhenDC3, 1,5-BisNPO, 2,7-BisNPN, and PhpC). (B) FRET-melting results ( $n = 3$ ) of experiments performed with F21T and increasing amounts (0–10 mol equiv) of the 6 compounds. Summary of the variations observed in the PAGE and FRET-melting assays performed with increasing amounts of the 6 compounds.

TPPS, 1,5-BisNPO, 2,7-BisNPN, and PhpC as possible destabilizers. To this end, we implemented *in vitro* assays previously used to characterize possible G4-unwinding agents, i.e., CD and PAGE. CD titrations were undertaken using the human telomeric G4-forming sequence (hTelo) and increasing amounts of candidates (1–10 mol equiv). CD titrations were systematically paralleled with UV–vis measurements to investigate the spectroscopic behavior of both the small molecule and its complex with hTelo in solution. As seen in Figures 4A and S11–19, we first confirmed the previous observations according to which TMPyP4 triggers a strong decrease (68.7%, at 10 mol equiv) of the CD signal of the G4 (collected at its maximum, 293 nm). However, the UV–vis

contribution of TMPyP4 alone (Figure 4B, blue dotted line) where the G4 absorbs light (collected at its maximum, 257 nm) is important and dose dependent, which also leads to an increase in the UV–vis contribution of the TMPyP4/hTelo complex (from 3.5% to 36.5% variation, Figure 4B, blue line), implying a possible induced CD (iCD) contribution to the CD signatures of the TMPyP4/hTelo complex. PhenDC3 does not disrupt the G4 structure (2.5% variation), while its UV–vis signatures are comparable to that of TMPyP4 (from –1.7% to 22.1% variation), implying again a possible iCD contribution. The UV–vis contribution of both TPPS and PhpC, alone or in complex with the G4, are comparatively low (from –4.1% to 13.0% for TPPS/hTelo and from –3.4% to 7.7% for PhpC/

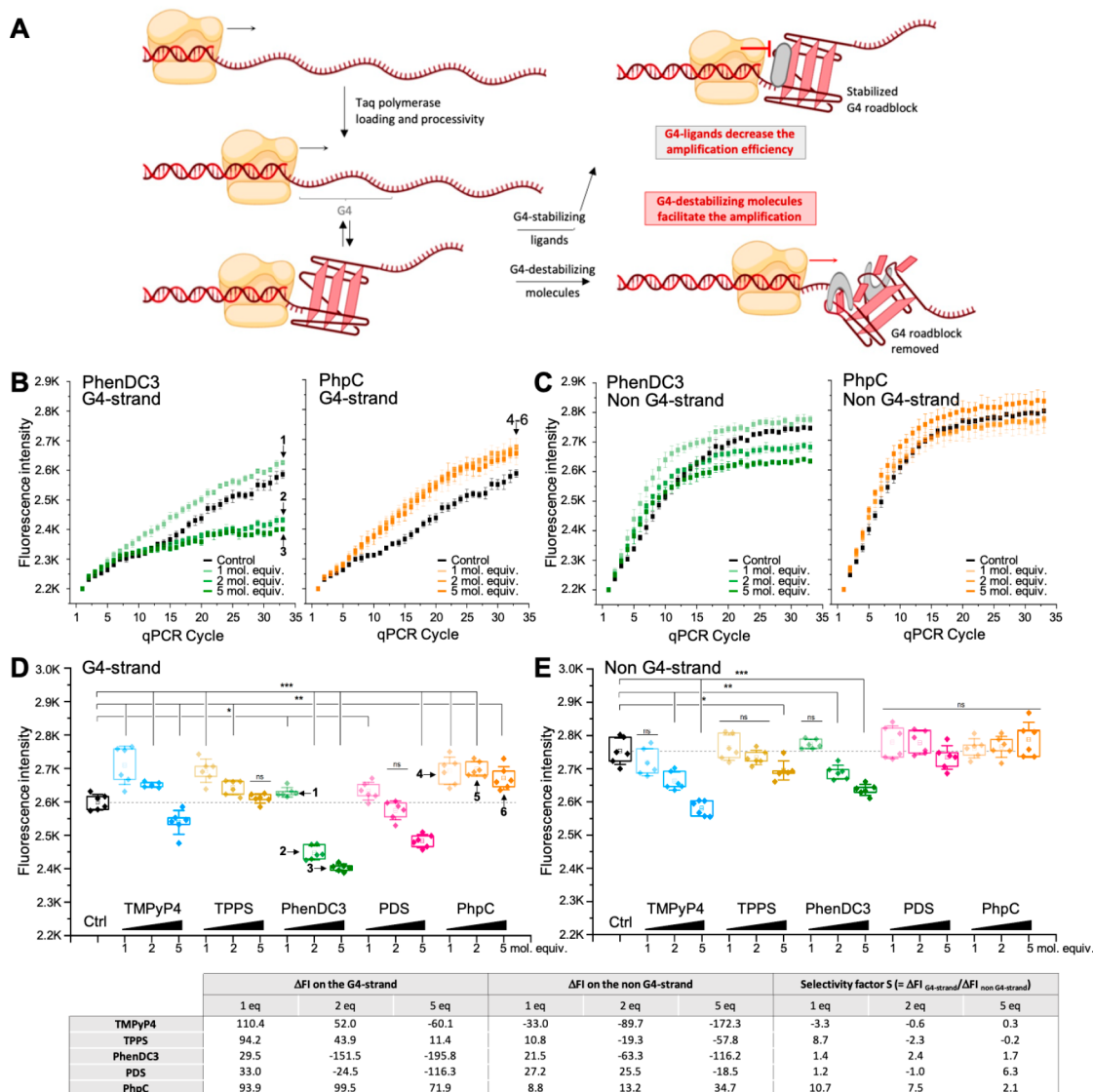


**Figure 6.** (A) Schematic representation of the qPCR stop assay developed by Sabouri et al.<sup>98</sup> Created with BioRender. (B and C) Examples of experimental curves ( $n = 3$ ) obtained for qPCR stop assay investigations performed with increasing amounts (1–5 mol equiv) of PhenDC3 and PhpC with either the G4-containing strand (B) or the control strand without G4 (non-G4 strand, C). (D and E) Results collected with 1–5 mol equiv of TMPyP4, TPPS, PhenDC3, PDS, and PhpC on both the G4-containing strand (D) and the control strand without G4 (non-G4 strand, E). Significance determined by two-sample  $t$  test: \*  $p < 0.01$ , \*\*  $p < 0.001$ , and \*\*\*  $p < 0.0001$ .

hTelo) while they significantly reduce the G4 structure bands in CD (down to  $-20.5\%$  and  $-17.5\%$ , respectively). The two azacyclophanes are found to reduce G4 signal in both CD ( $-27.3\%$  and  $-52.1\%$  for 1,5-BisNPO and 2,7-BisNPN, respectively) and UV-vis ( $-26.7\%$  and  $-20.5\%$ , respectively) with a minimal UV-vis contribution alone in solution. Collectively, these results highlight that great caution must be exercised when relying only on CD titrations to study DNA/small molecule interactions because of possible iCD contributions and other possible artefacts (e.g., aggregation, vide infra) that cannot be easily unraveled.

PAGE investigations were also performed with this series of 6 compounds, the partial unfolding of hTelo G4 being expected to result in smeared PAGE bands (originating in an unstructured shape, a bigger molecular volume, and a modified charge) rather than in loss of the signal (Figure S20). As above, TMPyP4 triggers a strong decrease of the band corresponding to hTelo ( $-76.1\%$  at 20 mol equiv, Figure 5A), which is not in

line with the UV-vis titration ( $36.5\%$  increase at 10 mol equiv, Figure 4B) and might originate in aggregation/precipitation events. PhenDC3 leads to band disappearance to an even greater extent ( $-89.4\%$  at 20 mol equiv), again suggestive of possible aggregation/precipitation of the ligand/hTelo complex. Indeed, a ligand-mediated formation of multimeric G4s, or multimerization,<sup>92</sup> has been demonstrated for some G4 ligands (e.g., *N*-methyl-indoloquinolinium<sup>93</sup> and porphyrin)<sup>94</sup> and characterized both experimentally<sup>95</sup> and theoretically,<sup>96</sup> which can lead to supramolecular assemblies too large to migrate within the gel lattice. In these conditions, TPPS is found to be rather inactive (from  $1.4\%$  to  $-4.7\%$  variation), while the two azacyclophanes and PhpC provide dose-dependent responses (from  $2.2\%$  to  $-49.3\%$  for 1,5-BisNPO,  $3.1\%$  to  $-41.7\%$  for 2,7-BisNPN, and  $-0.6\%$  to  $-13.1\%$  for PhpC), in line with the CD/UV-vis results. These properties were further studied by dynamic light scattering (DLS) experiments performed with both TMPyP4 and PhpC (Figure

S21). DLS confirmed the ability of TMPyP4 to disrupt G4 organization at a low DNA:ligand ratio (in line with the results seen in Figure 4) but trigger the formation of large-size aggregates at a higher ratio (1:5). DLS also confirmed that PhpC decreases the hydrodynamic diameter of the particles in solution in a dose–response manner (in line with results seen in Figure 4).

Finally, the apparent affinity of these candidates for hTelo was evaluated using the classical FRET-melting assay (with the doubly labeled hTelo, F21T).<sup>97</sup> As seen in Figures S5B and S22–24, this stabilization is quite high and dose dependent for PhenDC3 and 2,7-BisNPN ( $\Delta T_{1/2}$  up to 30.9 and 13.8 °C at 10 mol equiv, respectively), while saturation is obtained at 5 mol equiv of TMPyP4 ( $\Delta T_{1/2} = 19.9$  °C). Conversely, TPPS, 1,5-BisNPO, and PhpC do not display any affinity for F21T and are even able to lower its melting temperature by 1.6, 0.2, and 1.4 °C, respectively. These results thus show that 3 candidates display high affinity for folded G4s (TMPyP4, PhenDC3, and 2,7-BisNPN), while TPPS, 1,5-BisNPO, and PhpC do not interact with folded G4s.

Altogether, the wealth of data collected through this in vitro workflow indicates that each of these techniques provides interesting insights into the G4-interacting properties of the tested candidates but cannot be used and trusted independently. Only the combination of complementary techniques (fluorescence- versus absorbance-based assays, isothermal versus variable-temperature experiments, etc.) gives reliable information on the actual G4-interacting properties of these candidates. Here, PhpC passes all tests (TPPS being discarded at the PAGE step, 1,5-BisNPO at the CD/UV–vis step, and 2,7-BisNPN at the FRET-melting step), making it suited to be evaluated through additional experiments, notably in the presence of enzymes (vide infra). Before that, we tried to obtain more direct insights into the way it interacts with G4s by both NMR and fluorescence investigations. The former was poorly conclusive (Figure S25) owing to the overall decrease of the NMR signals of hTelo rather than a clear NMR signal redistribution. The latter (Figure S26) lends credence to the hypothesis that PhpC might be able to trap a transiently flipping guanine (Figure 2B). Indeed, PhpC fluorescence is sensitive to the proximity of nucleobases. This was exploited to monitor the association of a PNA (peptidic nucleic acid) strand it belongs to with a target DNA strand via fluorescence quenching.<sup>88,89</sup> We first titrated PhpC against guanosine monophosphate (GMP, 1–5 mol equiv) to mimic a flipping G, but its fluorescence was only marginally affected (–7.0%). This indicates that the formation of the PhpC:GMP base pair *se* does not influence the spectroscopic properties of the cytosine derivative. We then titrated PhpC against hTelo and found that decreasing the G4 stability by decreasing the  $K^+$  concentration of the buffer (from 100 to 1 mM  $K^+$ ) triggers a notable decrease of the PhpC fluorescence (–25.1%, –30.5%, and –36.4% for 100, 10, and 1 mM  $K^+$ , respectively; the relationship between G4 stability ( $T_{1/2}$ ) and fluorescence quenching as a function of the  $K^+$  content is near linear ( $R^2 = 0.96$ )). The decrease of the PhpC fluorescence is thus attributed to the transient opening of the external G-quartet (the external G-quartet breathes more easily in a less stable G4), enabling PhpC to trap a flipping G, thus laying in close proximity of the remaining G-triad that can affect its fluorescence by contact quenching (schematically represented in Figure S26).

### PhpC Favors Enzyme Processivity via G4 Disruption.

This putative binding mode makes PhpC compatible with enzymatic processivity. Indeed, PhpC might help enzymes translocation through G4 motifs by decreasing the G4 stability, transiently stabilizing a partially open G4 via weak and reversible interactions only (H bonds) with the wobbling G. To investigate this, the complete Pif1 helicase assay described in Figure 2A was implemented at different enzyme concentrations (140–170 nM) in the absence or presence of 10 mol equiv of either PhpC or TMPyP4 (Figure S27). Quite satisfyingly, the presence of PhpC enhances the Pif1-mediated G4 unfolding (between 1.5- and 2.4-fold), while TMPyP4 decreases the unfolding efficiency (0.6-fold), in line with the results obtained with all other G4 ligands evaluated so far.<sup>90</sup>

To go a step further, we revisited the qPCR stop assay recently developed by Sabouri et al. that involves the *Taq* DNA polymerase (Figure 6A).<sup>98</sup> This assay relies on the amplification of a 97-nt-long strand comprised of a central G4-forming sequence (so-called G4 strand) and of its complementary strand as the control (so-called non-G4 strand). A folded G4 acts as a roadblock to *Taq*,<sup>99,100</sup> which stalls replication and leads to a decreased amplification efficiency, quantified here by qPCR measurements (expressed as SYBR Green fluorescence intensity (FI), or  $\Delta FI$  when compared to the control, in arbitrary unit, a.u.): the G4 stabilizer PhenDC3 was described to foster this effect.<sup>98</sup> We thus reasoned that G4 unwinders might conversely increase the amplification efficiency. Importantly, the commercial availability of *Taq* enables a wider range of experiments, including dose–response investigations (1, 2 and 5 mol equiv), with both G4- and non-G4-forming oligonucleotides.

We first confirmed that increasing amounts of PhenDC3 decreases the efficiency of the amplification of the G4 strand ( $\Delta FI$  down to –195.8 at 5 mol equiv, Figures 6B, 6D, and S28, Table S3), in line with what was described by Sabouri.<sup>98</sup> The other established G4 ligand PDS operates the same way ( $\Delta FI$  down to –116.3). TPPS and PhpC were both found to improve the amplification, with a better overall activity for PhpC ( $\Delta FI$  between 71.9 and 93.9, Figure 6B and 6D) as a high DNA:TPPS ratio tends to diminish the effect of TPPS ( $\Delta FI = 94.2, 43.9,$  and  $11.4$  at 1, 2, and 5 mol equiv, respectively, Figure 6B and 6D).

Interestingly, TMPyP4 aids amplification at a low DNA:ligand ratio ( $\Delta FI = 110.4$  at 1 mol equiv) but inhibits it at higher ratio ( $\Delta FI$  down to –60.1 at 5 mol equiv), in full agreement with the results described above and obtained via alternative techniques. Experiments performed with the non-G4 strand (Figures 6C, 6E, and S29) confirmed the indiscriminate DNA binding properties of both TMPyP4, with a selectivity factor  $S$  (defined as  $S = \Delta FI_{G4} / \Delta FI_{non-G4}$ ) between 0.3 and –3.3, and, more surprisingly, PhenDC3 ( $S$  between 1.4 and 2.4), as described by Sabouri.<sup>98</sup> They also demonstrate the excellent G4 selectivity of the G4 ligand PDS ( $S$  up to 8.3) and of the G4 unwinders TPPS and PhpC ( $S$  up to 8.7 and 10.7, respectively).

Altogether, the results collected with both the G4-helicase Pif1 and the DNA polymerase *Taq* further demonstrate the ability of PhpC to unwind G4 according to a new approach, fully complementary to the 6 in vitro assays described above. These results thus open new horizons for chemical biology as they provide the first validated example of a small molecule able to facilitate G4-unwinding, thus offering new strategic opportunities for compensating for and/or rescuing G4-

helicase deficiencies at the origin of severe genetic dysfunctions and diseases.

## ■ CONCLUSION

The wealth of data collected here highlights the issues faced when exploring the ability of small molecules to disrupt G4s, as their behavior is found to be strongly dependent on the technique and the concentration used, as previously evoked.<sup>68</sup> This originates from the fact that small molecules can interact with G4s in many different ways, as confirmed here with TMPyP4, certainly the most representative example of a compound whose G4-stabilization/-disruption properties are complicated to unravel. Our results demonstrate the versatility of the porphyrins as DNA-interacting scaffolds as modification of their chemical core (here, their charge and side arms; previously their side arms<sup>68</sup> and the presence of a metal in their central cavity)<sup>67</sup> can reverse their binding properties. They also cast a bright light on the promising G-clamp analog scaffold PhpC whose ability to efficiently disrupt G4 structures and facilitate G4-helicase activity was thoroughly demonstrated *in vitro*.

Beyond this, our results lend credence to the reliability of a multistep methodology combining different techniques (G4-unfold, CD, UV-vis, PAGE, DLS, FRET-melting, G4-helicase assay, and qPCR stop assay) to assess the actual efficiency of putative G4-unwinding candidates in the most reliable way possible. These techniques are complementary as their intrinsic advantages and drawbacks can compensate for each other. For instance, the G4-unfold assay provides reliable tendencies (stabilization, destabilization, no effects) in a fast, practically convenient (easy preparation) and rather inexpensive manner (short synthetic oligonucleotides, no enzymes, routine spectrophotometers), but it somehow overestimates these tendencies, which can be corrected via normalization at the expense of the amplitude of the response. The CD and UV-vis titrations and DLS and PAGE experiments might be informative, but they are low-throughput assays and can, in addition, turn out to be tedious. Conversely, the FRET-melting technique is a high-throughput screen but it allows for the reliable identification of G4 stabilizers only. The G4-helicase assay suffers from the fastidious access to the Pif1 helicase, while the enzymatic mix required for the qPCR stop assay is commercially available (which makes it highly reproducible) but expensive, and its implementation could be long.

The ideal assay is still to be found, but the workflow described here is currently the best option. Strategically, our advice is to implement the two HTS assays (G4-unfold and qPCR stop assay) for the first selection step (ca. 20 compounds/day) and to further characterize the properties of the candidates via the other techniques, mainly to discard false positives. Applying this workflow to wider chemical libraries will undoubtedly lead to the identification of ever more efficient G4 unwinders, which soon will find applications as promising chemical biology tools in the field of genetic diseases.

## ■ ASSOCIATED CONTENT

### SI Supporting Information

The Supporting Information is available free of charge at <https://pubs.acs.org/doi/10.1021/jacs.1c04426>.

Preparation and sequences of the oligonucleotides used in this study; additional results obtained with the G4-

unfold assay during CD/UV-vis titrations, PAGE analysis, DLS investigations, FRET-melting assay, along with preliminary NMR results, fluorescence titrations, additional Pif1 helicase assay results, and qPCR stop assay results (PDF)

## ■ AUTHOR INFORMATION

### Corresponding Author

David Monchaud – *Institut de Chimie Moléculaire, ICMUB CNRS UMR 6302, UBFC, 21078 Dijon, France*;  
orcid.org/0000-0002-3056-9295;  
Email: david.monchaud@cnrs.fr

### Authors

Jérémie Mitteaux – *Institut de Chimie Moléculaire, ICMUB CNRS UMR 6302, UBFC, 21078 Dijon, France*

Pauline Lejault – *Institut de Chimie Moléculaire, ICMUB CNRS UMR 6302, UBFC, 21078 Dijon, France*

Filip Wojciechowski – *Department of Chemistry, The University of Western Ontario, London, Ontario N6A 5B7, Canada*

Alexandra Joubert – *Genome Structure and Instability Laboratory, CNRS UMR 7196, INSERM U1154, National Museum of Natural History, Alliance Sorbonne Université, 75005 Paris, France*

Julien Boudon – *Laboratoire Interdisciplinaire Carnot de Bourgogne, ICB CNRS UMR 6303, UBFC, 21078 Dijon, France*; orcid.org/0000-0002-2500-5030

Nicolas Desbois – *Institut de Chimie Moléculaire, ICMUB CNRS UMR 6302, UBFC, 21078 Dijon, France*;  
orcid.org/0000-0002-1156-4608

Claude P. Gros – *Institut de Chimie Moléculaire, ICMUB CNRS UMR 6302, UBFC, 21078 Dijon, France*;  
orcid.org/0000-0002-6966-947X

Robert H. E. Hudson – *Department of Chemistry, The University of Western Ontario, London, Ontario N6A 5B7, Canada*; orcid.org/0000-0002-6530-6479

Jean-Baptiste Boulé – *Genome Structure and Instability Laboratory, CNRS UMR 7196, INSERM U1154, National Museum of Natural History, Alliance Sorbonne Université, 75005 Paris, France*

Anton Granzhan – *Institut Curie, CNRS UMR 9187, INSERM U1196, PSL Research University, 91405 Orsay, France; Université Paris Saclay, CNRS UMR 9187, INSERM U1196, 91405 Orsay, France*; orcid.org/0000-0002-0424-0461

Complete contact information is available at:  
<https://pubs.acs.org/doi/10.1021/jacs.1c04426>

### Notes

The authors declare no competing financial interest.

## ■ ACKNOWLEDGMENTS

This work was supported by the CNRS (A.G. and D.M.), the INSERM Plan Cancer 2014–2019 (19CP117-00 for D.M.), the Agence Nationale de la Recherche (ANR-17-CE17-0010-01 for A.G. and D.M.), and the European Union (PO FEDER-FSE Bourgogne 2014/2020 programs, grant no. BG0021532). The authors are grateful to Marc Pirrotta (ICMUB) for fluorescence investigations.

## ■ REFERENCES

- (1) Rhodes, D.; Lipps, H. J. G-quadruplexes and their regulatory roles in biology. *Nucleic Acids Res.* **2015**, *43* (18), 8627–8637.
- (2) Varshney, D.; Spiegel, J.; Zyner, K.; Tannahill, D.; Balasubramanian, S. The regulation and functions of DNA and RNA G-quadruplexes. *Nat. Rev. Mol. Cell Biol.* **2020**, *21*, 459–474.
- (3) Raguseo, F.; Chowdhury, S.; Minard, A.; Di Antonio, M. Chemical-biology approaches to probe DNA and RNA G-quadruplex structures in the genome. *Chem. Commun.* **2020**, *56*, 1317–1324.
- (4) Spiegel, J.; Adhikari, S.; Balasubramanian, S. The structure and function of DNA G-quadruplexes. *Trends Chem.* **2020**, *2* (2), 123–136.
- (5) Mueller, S.; Kumari, S.; Rodriguez, R.; Balasubramanian, S. Small-molecule-mediated G-quadruplex isolation from human cells. *Nat. Chem.* **2010**, *2* (12), 1095–1098.
- (6) Renard, I.; Grandmougin, M.; Roux, A.; Yang, S. Y.; Lejault, P.; Pirrotta, M.; Wong, J. M. Y.; Monchaud, D. Small-molecule affinity capture of DNA/RNA quadruplexes and their identification in vitro and in vivo through the G4RP protocol. *Nucleic Acids Res.* **2019**, *47* (11), 5502–5510.
- (7) Chambers, V. S.; Marsico, G.; Boutell, J. M.; Di Antonio, M.; Smith, G. P.; Balasubramanian, S. High-throughput sequencing of DNA G-quadruplex structures in the human genome. *Nat. Biotechnol.* **2015**, *33* (8), 877–881.
- (8) Hänsel-Hertsch, R.; Beraldi, D.; Lensing, S. V.; Marsico, G.; Zyner, K.; Parry, A.; Di Antonio, M.; Pike, J.; Kimura, H.; Narita, M.; Tannahill, D.; Balasubramanian, S. G-quadruplex structures mark human regulatory chromatin. *Nat. Genet.* **2016**, *48* (10), 1267–1272.
- (9) Marsico, G.; Chambers, V. S.; Sahakyan, A. B.; McCauley, P.; Boutell, J. M.; Antonio, M. D.; Balasubramanian, S. Whole genome experimental maps of DNA G-quadruplexes in multiple species. *Nucleic Acids Res.* **2019**, *47* (8), 3862–3874.
- (10) Hänsel-Hertsch, R.; Simeone, A.; Shea, A.; Hui, W. W. I.; Zyner, K. G.; Marsico, G.; Rueda, O. M.; Bruna, A.; Martin, A.; Zhang, X.; Adhikari, S.; Tannahill, D.; Caldas, C.; Balasubramanian, S. Landscape of G-quadruplex DNA structural regions in breast cancer. *Nat. Genet.* **2020**, *52* (9), 878–883.
- (11) Umar, M. I.; Ji, D.; Chan, C.-Y.; Kwok, C. K. G-Quadruplex-Based Fluorescent Turn-On Ligands and Aptamers: From Development to Applications. *Molecules* **2019**, *24* (13), 2416.
- (12) Monchaud, D. Quadruplex detection in human cells. *Annu. Rep. Med. Chem.* **2020**, *54*, 133–160.
- (13) Hänsel-Hertsch, R.; Di Antonio, M.; Balasubramanian, S. DNA G-quadruplexes in the human genome: detection, functions and therapeutic potential. *Nat. Rev. Mol. Cell Biol.* **2017**, *18* (5), 279–284.
- (14) Kwok, C. K.; Merrick, C. J. G-quadruplexes: prediction, characterization, and biological application. *Trends Biotechnol.* **2017**, *35* (10), 997–1013.
- (15) Wang, G.; Vasquez, K. M. Impact of alternative DNA structures on DNA damage, DNA repair, and genetic instability. *DNA Repair* **2014**, *19*, 143–151.
- (16) Bryan, T. M. Mechanisms of DNA Replication and Repair: Insights from the Study of G-Quadruplexes. *Molecules* **2019**, *24* (19), 3439.
- (17) Zell, J.; Rota Sperti, F.; Britton, S.; Monchaud, D. DNA folds threaten genetic stability and can be leveraged for chemotherapy. *RSC Chem. Biol.* **2021**, *2*, 47–76.
- (18) Mirkin, E. V.; Mirkin, S. M. Replication fork stalling at natural impediments. *Microbiol. Mol. Biol. Rev.* **2007**, *71* (1), 13–35.
- (19) Mendoza, O.; Bourdoncle, A.; Boulé, J.-B.; Brosh, R. M.; Mergny, J.-L. G-quadruplexes and helicases. *Nucleic Acids Res.* **2016**, *44* (5), 1989–2006.
- (20) Lansdorp, P.; van Wietmarschen, N. Helicases FANCF, RTEL1 and BLM Act on Guanine Quadruplex DNA in Vivo. *Genes* **2019**, *10* (11), 870.
- (21) Lerner, L. K.; Sale, J. E. Replication of G quadruplex DNA. *Genes* **2019**, *10* (2), 95.
- (22) Brosh, R. M.; Matson, S. W. History of DNA Helicases. *Genes* **2020**, *11* (3), 255.
- (23) Lejault, P.; Mitteau, J.; Sperti, F. R.; Monchaud, D. How to untie G-quadruplex knots and why? *Cell Chem. Biol.* **2021**, *28*, 436–455.
- (24) Singleton, M. R.; Dillingham, M. S.; Wigley, D. B. Structure and mechanism of helicases and nucleic acid translocases. *Annu. Rev. Biochem.* **2007**, *76*, 23–50.
- (25) Fairman-Williams, M. E.; Guenther, U.-P.; Jankowsky, E. SF1 and SF2 helicases: family matters. *Curr. Opin. Struct. Biol.* **2010**, *20* (3), 313–324.
- (26) Ribeyre, C.; Lopes, J.; Boule, J.-B.; Piazza, A.; Guedin, A.; Zakian, V. A.; Mergny, J.-L.; Nicolas, A. The Yeast Pif1 Helicase Prevents Genomic Instability Caused by G-Quadruplex-Forming CEB1 Sequences In Vivo. *PLoS Genet.* **2009**, *5* (5), e1000475.
- (27) Piazza, A.; Boule, J.-B.; Lopes, J.; Mingo, K.; Largy, E.; Teulade-Fichou, M.-P.; Nicolas, A. Genetic instability triggered by G-quadruplex interacting Phen-DC compounds in *Saccharomyces cerevisiae*. *Nucleic Acids Res.* **2010**, *38* (13), 4337–4348.
- (28) Paeschke, K.; Capra, J. A.; Zakian, V. A. DNA Replication through G-Quadruplex Motifs Is Promoted by the *Saccharomyces cerevisiae* Pif1 DNA Helicase. *Cell* **2011**, *145* (5), 678–691.
- (29) Sun, H.; Karow, J. K.; Hickson, I. D.; Maizels, N. The Bloom's syndrome helicase unwinds G4 DNA. *J. Biol. Chem.* **1998**, *273* (42), 27587–27592.
- (30) Mohaghegh, P.; Karow, J. K.; Brosh, R. M.; Bohr, V. A.; Hickson, I. D. The Bloom's and Werner's syndrome proteins are DNA structure-specific helicases. *Nucleic Acids Res.* **2001**, *29* (13), 2843–2849.
- (31) Fry, M.; Loeb, L. A. Human Werner syndrome DNA helicase unwinds tetrahelical structures of the fragile X syndrome repeat sequence d(CGG)(n). *J. Biol. Chem.* **1999**, *274* (18), 12797–12802.
- (32) Wu, Y.; Shin-Ya, K.; Brosh, R. M., Jr. FANCF helicase defective in Fanconi anemia and breast cancer unwinds G-quadruplex DNA to defend genomic stability. *Mol. Cell Biol.* **2008**, *28* (12), 4116–4128.
- (33) London, T. B. C.; Barber, L. J.; Mosedale, G.; Kelly, G. P.; Balasubramanian, S.; Hickson, I. D.; Boulton, S. J.; Hiom, K. FANCF Is a Structure-specific DNA Helicase Associated with the Maintenance of Genomic G/C Tracts. *J. Biol. Chem.* **2008**, *283* (52), 36132–36139.
- (34) Wu, Y.; Sommers, J. A.; Khan, I.; de Winter, J. P.; Brosh, R. M., Jr. Biochemical Characterization of Warsaw Breakage Syndrome Helicase. *J. Biol. Chem.* **2012**, *287* (2), 1007–1021.
- (35) Bharti, S. K.; Sommers, J. A.; George, F.; Kuper, J.; Hamon, F.; Shin-Ya, K.; Teulade-Fichou, M.-P.; Kisker, C.; Brosh, R. M., Jr. Specialization among Iron-Sulfur Cluster Helicases to Resolve G-quadruplex DNA Structures That Threaten Genomic Stability. *J. Biol. Chem.* **2013**, *288* (39), 28217–28229.
- (36) Ellis, N. A.; Groden, J.; Ye, T.-Z.; Straughen, J.; Lennon, D. J.; Ciocci, S.; Proytcheva, M.; German, J. The Bloom's syndrome gene product is homologous to RecQ helicases. *Cell* **1995**, *83* (4), 655–666.
- (37) Yu, C.-E.; Oshima, J.; Fu, Y.-H.; Wijsman, E. M.; Hisama, F.; Alisch, R.; Matthews, S.; Nakura, J.; Miki, T.; Ouais, S.; et al. Positional cloning of the Werner's syndrome gene. *Science* **1996**, *272* (5259), 258–262.
- (38) Litman, R.; Peng, M.; Jin, Z.; Zhang, F.; Zhang, J. R.; Powell, S.; Andreassen, P. R.; Cantor, S. B. BACH1 is critical for homologous recombination and appears to be the Fanconi anemia gene product FANCF. *Cancer Cell* **2005**, *8* (3), 255–265.
- (39) Levan, O.; Attwooll, C.; Henry, R. T.; Milton, K. L.; Neveling, K.; Rio, P.; Batish, S. D.; Kalb, R.; Velleuer, E.; Barral, S.; et al. The BRCA1-interacting helicase BRIP1 is deficient in Fanconi anemia. *Nat. Genet.* **2005**, *37* (9), 931–933.
- (40) Levitus, M.; Waisfisz, Q.; Godthelp, B. C.; De Vries, Y.; Hussain, S.; Wiegant, W. W.; Elghalbzouri-Maghrani, E.; Steltenpool, J.; Rooimans, M. A.; Pals, G.; et al. The DNA helicase BRIP1 is defective in Fanconi anemia complementation group J. *Nat. Genet.* **2005**, *37* (9), 934–935.
- (41) van der Lelij, P.; Chrzanoska, K. H.; Godthelp, B. C.; Rooimans, M. A.; Oostra, A. B.; Stumm, M.; Zdzienicka, M. Ig. Z.;

- Joenje, H.; de Winter, J. P. Warsaw Breakage Syndrome, a Cohesinopathy Associated with Mutations in the XPD Helicase Family Member DDX11/ChIR1. *Am. J. Hum. Genet.* **2010**, *86* (2), 262–266.
- (42) Chisholm, K. M.; Aubert, S. D.; Freese, K. P.; Zakian, V. A.; King, M. C.; Welch, P. L. A Genomewide Screen for Suppressors of Alu-Mediated Rearrangements Reveals a Role for PIF1. *PLoS One* **2012**, *7* (2), e30748.
- (43) Moruno-Manchon, J. F.; Lejault, P.; Wang, Y.; McCauley, B.; Honarpisheh, P.; Morales Scheihing, D. A.; Singh, S.; Dang, W.; Kim, N.; Urayama, A.; et al. Small-molecule G-quadruplex stabilizers reveal a novel pathway of autophagy regulation in neurons. *eLife* **2020**, *9*, No. e52283.
- (44) Neidle, S. Quadruplex Nucleic Acids as Novel Therapeutic Targets. *J. Med. Chem.* **2016**, *59* (13), 5987–6011.
- (45) Sun, D. Y.; Thompson, B.; Cathers, B. E.; Salazar, M.; Kerwin, S. M.; Trent, J. O.; Jenkins, T. C.; Neidle, S.; Hurley, L. H. Inhibition of human telomerase by a G-quadruplex-interactive compound. *J. Med. Chem.* **1997**, *40* (14), 2113–2116.
- (46) O'Hagan, M. P.; Morales, J. C.; Galan, M. C. Binding and Beyond: What Else Can G-Quadruplex Ligands Do? *Eur. J. Org. Chem.* **2019**, No. 31–32, 4995–5017.
- (47) del Mundo, I. M.; Vasquez, K. M.; Wang, G. Modulation of DNA structure formation using small molecules. *Biochim. Biophys. Acta, Mol. Cell Res.* **2019**, *1866*, 118539.
- (48) Weisman-Shomer, P.; Cohen, E.; Hershco, I.; Khateb, S.; Wolfowitz-Barchad, O.; Hurley, L. H.; Fry, M. The cationic porphyrin TMPyP4 destabilizes the tetraplex form of the fragile X syndrome expanded sequence d (CGG)<sub>n</sub>. *Nucleic Acids Res.* **2003**, *31* (14), 3963–3970.
- (49) Ofer, N.; Weisman-Shomer, P.; Shklover, J.; Fry, M. The quadruplex r (CGG)<sub>n</sub> destabilizing cationic porphyrin TMPyP4 cooperates with hnRNPs to increase the translation efficiency of fragile X premutation mRNA. *Nucleic Acids Res.* **2009**, *37* (8), 2712–2722.
- (50) Zamiri, B.; Reddy, K.; Macgregor, R. B.; Pearson, C. E. TMPyP4 porphyrin distorts RNA G-quadruplex structures of the disease-associated r (GGGGCC)<sub>n</sub> repeat of the C9orf72 gene and blocks interaction of RNA-binding proteins. *J. Biol. Chem.* **2014**, *289* (8), 4653–4659.
- (51) Joachimi, A.; Mayer, G.; Hartig, J. S. A new anticoagulant-antidote pair: Control of thrombin activity by aptamers and porphyrins. *J. Am. Chem. Soc.* **2007**, *129* (11), 3036–3037.
- (52) Kaluzhny, D.; Ilyinsky, N.; Shchekotikhin, A.; Sinkevich, Y.; Tsvetkov, P. O.; Tsvetkov, V.; Veselovsky, A.; Livshits, M.; Borisova, O.; Shtil, A.; Shchyolkina, A. Disordering of Human Telomeric G-Quadruplex with Novel Antiproliferative Anthrathiophenedione. *PLoS One* **2011**, *6* (11), No. e27151.
- (53) Waller, Z. A. E.; Sewitz, S. A.; Hsu, S.-T. D.; Balasubramanian, S. A Small Molecule That Disrupts G-Quadruplex DNA Structure and Enhances Gene Expression. *J. Am. Chem. Soc.* **2009**, *131* (35), 12628–12633.
- (54) O'Hagan, M. P.; Haldar, S.; Duchi, M.; Oliver, T. A.; Mulholland, A. J.; Morales, J. C.; Galan, M. C. A Photoresponsive Stiff-Stilbene Ligand Fuels the Reversible Unfolding of G-Quadruplex DNA. *Angew. Chem.* **2019**, *131* (13), 4378–4382.
- (55) Monchaud, D.; Yang, P.; Lacroix, L.; Teulade-Fichou, M.-P.; Mergny, J.-L. A metal-mediated conformational switch controls G-quadruplex binding affinity. *Angew. Chem., Int. Ed.* **2008**, *47* (26), 4858–4861.
- (56) Rajczak, E.; Gluszynska, A.; Juskowiak, B. Interaction of metallacrown complexes with G-quadruplex DNA. *J. Inorg. Biochem.* **2016**, *155*, 105–114.
- (57) Smirnov, I. V.; Shafer, R. H. Electrostatics dominate quadruplex stability. *Biopolymers* **2007**, *85* (1), 91–101.
- (58) Ueda, Y.-m.; Zouzumi, Y.-k.; Maruyama, A.; Nakano, S.-i.; Sugimoto, N.; Miyoshi, D. Effects of trimethylamine N-oxide and urea on DNA duplex and G-quadruplex. *Sci. Technol. Adv. Mater.* **2016**, *17* (1), 753–759.
- (59) Sun, H.; Xiang, J.; Liu, Y.; Li, L.; Li, Q.; Xu, G.; Tang, Y. A stabilizing and denaturing dual-effect for natural polyamines interacting with G-quadruplexes depending on concentration. *Biochimie* **2011**, *93* (8), 1351–1356.
- (60) Anantha, N. V.; Azam, M.; Sheardy, R. D. Porphyrin binding to quadruplexed T(4)G(4). *Biochemistry* **1998**, *37* (9), 2709–2714.
- (61) Siddiqui-Jain, A.; Grand, C. L.; Bearss, D. J.; Hurley, L. H. Direct evidence for a G-quadruplex in a promoter region and its targeting with a small molecule to repress c-MYC transcription. *Proc. Natl. Acad. Sci. U. S. A.* **2002**, *99* (18), 11593–11598.
- (62) Han, F. X. G.; Wheelhouse, R. T.; Hurley, L. H. Interactions of TMPyP4 and TMPyP2 with quadruplex DNA. Structural basis for the differential effects on telomerase inhibition. *J. Am. Chem. Soc.* **1999**, *121* (15), 3561–3570.
- (63) Alniss, H.; Zamiri, B.; Khalaj, M.; Pearson, C. E.; Macgregor Jr, R. B. Thermodynamic and spectroscopic investigations of TMPyP4 association with guanine- and cytosine-rich DNA and RNA repeats of C9orf72. *Biochem. Biophys. Res. Commun.* **2018**, *495* (4), 2410–2417.
- (64) Dutikova, Y. V.; Borisova, O.; Shchyolkina, A.; Lin, J.; Huang, S.; Shtil, A.; Kaluzhny, D. S, 10, 15, 20-Tetra-(N-methyl-3-pyridyl) porphyrin destabilizes the antiparallel telomeric quadruplex d (TTAGGG)<sub>4</sub>. *Mol. Biol.* **2010**, *44* (5), 823–831.
- (65) Li, F.; Tan, W.; Chen, H.; Zhou, J.; Xu, M.; Yuan, G. Up- and downregulation of mature miR-1587 function by modulating its G-quadruplex structure and using small molecules. *Int. J. Biol. Macromol.* **2019**, *121*, 127–134.
- (66) Simko, E. A.; Liu, H.; Zhang, T.; Velasquez, A.; Teli, S.; Haeusler, A. R.; Wang, J. G-quadruplexes offer a conserved structural motif for NONO recruitment to NEAT1 architectural lncRNA. *Nucleic Acids Res.* **2020**, *48* (13), 7421–7438.
- (67) Bhattacharjee, A. J.; Ahluwalia, K.; Taylor, S.; Jin, O.; Nicoludis, J. M.; Buscaglia, R.; Brad Chaires, J.; Kornfilt, D. J.P.; Marquardt, D. G.S.; Yatsunyk, L. A. Induction of G-quadruplex DNA structure by Zn(II) 5,10,15,20-tetrakis(N-methyl-4-pyridyl)porphyrin. *Biochimie* **2011**, *93*, 1297–1309.
- (68) D'Urso, A.; Randazzo, R.; Rizzo, V.; Gangemi, C.; Romanucci, V.; Zarrelli, A.; Tomaselli, G.; Milardi, D.; Borbone, N.; Purrello, R.; et al. Stabilization vs. destabilization of G-quadruplex superstructures: The role of the porphyrin derivative having spermine arms. *Phys. Chem. Chem. Phys.* **2017**, *19* (26), 17404–17410.
- (69) Murat, P.; Singh, Y.; Defrancq, E. Methods for investigating G-quadruplex DNA/ligand interactions. *Chem. Soc. Rev.* **2011**, *40* (11), 5293–5307.
- (70) Jaumot, J.; Gargallo, R. Experimental Methods for Studying the Interactions between G-Quadruplex Structures and Ligands. *Curr. Pharm. Des.* **2012**, *18* (14), 1900–1916.
- (71) Laguerre, A.; Chang, Y.; Pirrotta, M.; Desbois, N.; Gros, C. P.; Lesniewska, E.; Monchaud, D. Surface-promoted aggregation of amphiphilic quadruplex ligands drives their selectivity for alternative DNA structures. *Org. Biomol. Chem.* **2015**, *13* (25), 7034–7039.
- (72) Diabate, P. D.; Laguerre, A.; Pirrotta, M.; Desbois, N.; Boudon, J.; Gros, C. P.; Monchaud, D. DNA structure-specific sensitization of a metalloporphyrin leads to an efficient in vitro quadruplex detection molecular tool. *New J. Chem.* **2016**, *40* (7), 5683–5689.
- (73) Jiang, X.; Gros, C. P.; Chang, Y.; Desbois, N.; Zeng, L.; Cui, Y.; Kadish, K. M. Tetracationic and tetraanionic manganese porphyrins: electrochemical and spectroelectrochemical characterization. *Inorg. Chem.* **2017**, *56* (14), 8045–8057.
- (74) De Cian, A.; DeLemos, E.; Mergny, J.-L.; Teulade-Fichou, M.-P.; Monchaud, D. Highly efficient G-quadruplex recognition by bisquinolinium compounds. *J. Am. Chem. Soc.* **2007**, *129* (7), 1856–1857.
- (75) De Cian, A.; Cristofari, G.; Reichenbach, P.; De Lemos, E.; Monchaud, D.; Teulade-Fichou, M.-P.; Shin-Ya, K.; Lacroix, L.; Lingner, J.; Mergny, J.-L. Reevaluation of telomerase inhibition by quadruplex ligands and their mechanisms of action. *Proc. Natl. Acad. Sci. U. S. A.* **2007**, *104* (44), 17347–17352.
- (76) Rodriguez, R.; Mueller, S.; Yeoman, J. A.; Trentesaux, C.; Riou, J.-F.; Balasubramanian, S. A Novel Small Molecule That Alters

- Shelterin Integrity and Triggers a DNA-Damage Response at Telomeres. *J. Am. Chem. Soc.* **2008**, *130* (47), 15758–15758.
- (77) Rodriguez, R.; Miller, K. M.; Forment, J. V.; Bradshaw, C. R.; Nikan, M.; Britton, S.; Oelschlaegel, T.; Xhemalce, B.; Balasubramanian, S.; Jackson, S. P. Small-molecule-induced DNA damage identifies alternative DNA structures in human genes. *Nat. Chem. Biol.* **2012**, *8* (3), 301–310.
- (78) Read, M.; Harrison, R. J.; Romagnoli, B.; Taniou, F. A.; Gowan, S. H.; Reszka, A. P.; Wilson, W. D.; Kelland, L. R.; Neidle, S. Structure-based design of selective and potent G quadruplex-mediated telomerase inhibitors. *Proc. Natl. Acad. Sci. U. S. A.* **2001**, *98* (9), 4844–4849.
- (79) Harrison, R. J.; Cuesta, J.; Chessari, G.; Read, M. A.; Basra, S. K.; Reszka, A. P.; Morrell, J.; Gowan, S. M.; Incles, C. M.; Taniou, F. A.; Wilson, W. D.; Kelland, L. R.; Neidle, S. Trisubstituted acridine derivatives as potent and selective telomerase inhibitors. *J. Med. Chem.* **2003**, *46* (21), 4463–4476.
- (80) Moore, M. J. B.; Schultes, C. M.; Cuesta, J.; Cuenca, F.; Gunaratnam, M.; Taniou, F. A.; Wilson, W. D.; Neidle, S. Trisubstituted acridines as G-quadruplex telomere targeting agents. Effects of extensions of the 3,6- and 9-side chains on quadruplex binding, telomerase activity, and cell proliferation. *J. Med. Chem.* **2006**, *49* (2), 582–599.
- (81) Mela, I.; Kranaster, R.; Henderson, R. M.; Balasubramanian, S.; Edwardson, J. M. Demonstration of Ligand Decoration, and Ligand-Induced Perturbation, of G-Quadruplexes in a Plasmid Using Atomic Force Microscopy. *Biochemistry* **2012**, *51* (2), 578–585.
- (82) Bahr, M.; Gabelica, V.; Granzhan, A.; Teulade-Fichou, M.-P.; Weinhold, E. Selective recognition of pyrimidine-pyrimidine DNA mismatches by distance-constrained macrocyclic bis-intercalators. *Nucleic Acids Res.* **2008**, *36* (15), 5000–5012.
- (83) Granzhan, A.; Largy, E.; Saettel, N.; Teulade-Fichou, M. P. Macrocyclic DNA-Mismatch-Binding Ligands: Structural Determinants of Selectivity. *Chem. - Eur. J.* **2010**, *16* (3), 878–889.
- (84) Paris, T.; Vigneron, J.-P.; Lehn, J.-M.; Cesario, M.; Guilhem, J.; Pascard, C. Molecular recognition of anionic substrates. Crystal structures of the supramolecular inclusion complexes of terephthalate and isophthalate dianions with a bis-intercaland receptor molecule. *J. Inclusion Phenom. Mol. Recognit. Chem.* **1999**, *33* (2), 191–202.
- (85) Jourdan, M.; Garcia, J.; Lhomme, J.; Teulade-Fichou, M.-P.; Vigneron, J.-P.; Lehn, J.-M. Threading Bis-Intercalation of a Macrocyclic Bisacridine at Abasic Sites in DNA: Nuclear Magnetic Resonance and Molecular Modeling Study. *Biochemistry* **1999**, *38* (43), 14205–14213.
- (86) Cudic, P.; Vigneron, J.-P.; Lehn, J.-M.; Cesario, M.; Prangé, T. Molecular Recognition of Azobenzene Dicarboxylates by Acridine-Based Receptor Molecules; Crystal Structure of the Supramolecular Inclusion Complex of trans-3,3'-Azobenzene Dicarboxylate with a Cyclo-bis-intercaland Receptor. *Eur. J. Org. Chem.* **1999**, No. 10, 2479–2484.
- (87) Lin, K.-Y.; Matteucci, M. D. A cytosine analogue capable of clamp-like binding to a guanine in helical nucleic acids. *J. Am. Chem. Soc.* **1998**, *120* (33), 8531–8532.
- (88) Wojciechowski, F.; Hudson, R. H. E. Fluorescence and Hybridization Properties of Peptide Nucleic Acid Containing a Substituted Phenylpyrrolocytosine Designed to Engage Guanine with an Additional H-Bond. *J. Am. Chem. Soc.* **2008**, *130* (38), 12574–12575.
- (89) Wojciechowski, F.; Hudson, R. H. E. Peptide Nucleic Acid Containing a Meta-Substituted Phenylpyrrolocytosine Exhibits a Fluorescence Response and Increased Binding Affinity toward RNA. *Org. Lett.* **2009**, *11* (21), 4878–4881.
- (90) Mendoza, O.; Gueddouda, N. M.; Boulé, J.-B.; Bourdoncle, A.; Mergny, J.-L. A fluorescence-based helicase assay: application to the screening of G-quadruplex ligands. *Nucleic Acids Res.* **2015**, *43*, e71.
- (91) Bertrand, H.; Granzhan, A.; Monchaud, D.; Saettel, N.; Guillot, R.; Clifford, S.; Guedin, A.; Mergny, J.-L.; Teulade-Fichou, M.-P. Recognition of G-Quadruplex DNA by Triangular Star-Shaped Compounds: With or Without Side Chains? *Chem. - Eur. J.* **2011**, *17* (16), 4529–4539.
- (92) Kolesnikova, S.; Curtis, E. A. Structure and function of multimeric G-quadruplexes. *Molecules* **2019**, *24* (17), 3074.
- (93) Funke, A.; Karg, B.; Dickerhoff, J.; Balke, D.; Müller, S.; Weisz, K. Ligand-Induced Dimerization of a Truncated Parallel MYC G-Quadruplex. *ChemBioChem* **2018**, *19* (5), 505–512.
- (94) Cheng, Y.; Cheng, M.; Hao, J.; Jia, G.; Monchaud, D.; Li, C. The noncovalent dimerization of a G-quadruplex/hemin DNAzyme improves its biocatalytic properties. *Chem. Sci.* **2020**, *11* (33), 8846–8853.
- (95) Haider, S. M.; Neidle, S.; Parkinson, G. N. A structural analysis of G-quadruplex/ligand interactions. *Biochimie* **2011**, *93* (8), 1239–1251.
- (96) Haider, S.; Parkinson, G. N.; Neidle, S. Molecular dynamics and principal components analysis of human telomeric quadruplex multimers. *Biophys. J.* **2008**, *95* (1), 296–311.
- (97) De Rache, A.; Mergny, J.-L. Assessment of selectivity of G-quadruplex ligands via an optimized FRET melting assay. *Biochimie* **2015**, *115*, 194–202.
- (98) Jamroskovic, J.; Obi, I.; Movahedi, A.; Chand, K.; Chorell, E.; Sabouri, N. Identification of putative G-quadruplex DNA structures in *S. pombe* genome by quantitative PCR stop assay. *DNA Repair* **2019**, *82*, 102678.
- (99) Han, H.; Hurley, L. H.; Salazar, M. A DNA polymerase stop assay for G-quadruplex-interactive compounds. *Nucleic Acids Res.* **1999**, *27* (2), 537–542.
- (100) Qin, Y.; Rezler, E. M.; Gokhale, V.; Sun, D.; Hurley, L. H. Characterization of the G-quadruplexes in the duplex nuclease hypersensitive element of the PDGF-A promoter and modulation of PDGF-A promoter activity by TMPyP4. *Nucleic Acids Res.* **2007**, *35* (22), 7698–7713.